On a particle tracking technique to predict disinfection in drinking water treatment systems.

B.A. Wols[*,1,2], J.A.M.H. Hofman[1,2], W.S.J. Uijttewaal[2], J.C. van Dijk[2].

[1] KWR Watercylce Research Institute
[2] Delft University of Technology
[*] Corresponding author: Groningenhaven 7, 3430 BB Niewegein, The Netherlands, bas.wols@kwrwater.nl

Abstract

Disinfection of drinking water is required to prevent the outbreak of water-borne diseases. Different treatment steps are available to disinfect the water, such as chlorination, ozonation or UV irradiation. The hydrodynamics of these processes play an important role in their performance. COMSOL Multiphysics was used to simulate the water flow in disinfection installations. Moreover, a particle tracking routine using the resolved flow fields from the COMSOL simulation was developed to calculate the movements of individual micro-organisms. The main advantage of a particle tracking (Lagrangian) method over an Eulerian method is that different quantities can be recorded for every particle, resulting in higher-order statistics for the desired quantity. The accuracy of a particle tracking method, however, is a point of concern. Special attention is needed to prevent particles from, unrealistically, accumulating at regions with low diffusion and to prevent them from virtually crossing the walls. The theory of stochastic differential equations was used to find the appropriate particle displacement equations that represent the advection-diffusion process.
The particle tracking technique was used to predict the disinfection in ozone contactors. By recording the amount of dissolved ozone exposed to each particle, a distribution of ozone exposures (CT-values) was obtained. The lowest CT-values are critical for disinfection. By changing the geometry – adding horizontal baffles or turning vanes – the lowest CT-values are increased, resulting in a more efficient design of ozone contactors.

Introduction

Disinfection of drinking water is required to prevent the outbreak of water-borne diseases. The disinfection aims to inactivate the micro-organisms, so that they can no longer infect humans. Different treatment steps are available to disinfect the water, such as chlorination, ozonation or UV irradiation. The hydrodynamics of these processes play an important role in their performance. Ongoing development of computers and software technology allows detailed modelling of the water flow through reactors and the influence of the water flow on physical, chemical and microbiological processes taking place within them. COMSOL Multiphysics was used to simulate the water flow in disinfection installations. Moreover, a particle tracking routine using the resolved flow fields from the COMSOL simulation was developed to calculate the movements of individual micro-organisms (bacteria, viruses etc.).

For predicting disinfection processes, transport and mixing mechanisms of chemical and microbial species are important. The main advantage of a particle tracking (Lagrangian) method over an Eulerian method is that different quantities (e.g., residence time, ozone exposure) can be recorded for every particle, resulting in higher-order statistics for the desired quantity. The accuracy of a particle tracking method, however, is a point of concern (Zhang et al., 2007). A thorough examination of different particle tracking methods is therefore conducted and specific problems are addressed. For example, special attention is needed to prevent particles from, unrealistically, accumulating at regions with low diffusion and to prevent them from virtually crossing the walls, which is in practice not possible of course. The particles were assumed to represent micro-organisms or micropollutants that move entirely with the fluid (particles without gravity, drag or lift forces). This approach is allowed if particles have a density close to the density of the fluid, and if they are smaller than the Kolmogorov length scales (~10^{-4} m), so that the velocity of the particle is the same as the fluid velocity (Baldyga and Orciuch, 2001), which is valid for micro-organisms in water (for example, one of the larger micro-organisms, *Bacillus subtilis* spores, has a length of 1-5 μm). The theory of stochastic differential equations was used to find the appropriate particle displacement equations that represent the

advection-diffusion process. The particle displacement was divided into an advection part and a diffusion part. From the theory of stochastic differential equations, numerical schemes were explored that modelled the diffusion of particles by random displacements accurately. The particle tracking scheme was tested for a channel flow.

2. Materials and methods

2.1 Stochastic differential equations

The molecular motion of small-sized bodies, suspended in a liquid, is called Brownian motion, discovered by Brown (1829), and is further explained by Einstein (1905). Langevin and others tried to formulate the Brownian motion process in terms of differential equations, written as:

$$dX_t = f(t, X_t)dt + g(t, X_t)dW_t \qquad X_t(0) = X_0 \tag{1}$$

where X_t is a stochastic variable and dW_t represents a random increment. The function $f(t, X_t)$ represents a drift term and $g(t,X_t)$ a noise term. This equation is known as a stochastic differential equation (sde) and requires a different approach than deterministic differential equations (Risken, 1984).
The increments dW_t are usually Gaussian with zero mean and a variance equal to dt. The increments can be generated by a Gaussian random number generator (with mean zero and variance 1):

$$\Delta W_t = N(0,1)\sqrt{\Delta t} \tag{2}$$

So the increment ΔW_t is a normal distributed random variable with mean zero and variance Δt. Instead of using a Gaussian distribution, which resulted in a Gaussian white noise process, we also investigated the use of a uniform distribution, which resulted in a uniform white noise process. The increments were then generated by a uniform random number generator (with mean zero and variance 1).

The particle tracking routine must obey the advection-diffusion equation, which is given by:

$$\frac{\partial C}{\partial t} + u_i \frac{\partial C}{\partial x_i} = \frac{\partial C}{\partial x_i}\left(D_{ij} \frac{\partial C}{\partial x_j} \right) \tag{3}$$

using the Einstein summation convention (terms with a repeating index are summed up).

Assuming an isotropic homogeneous diffusion process, the diffusion matrix reduces to:

$$D_{ij} = \begin{pmatrix} D & 0 \\ 0 & D \end{pmatrix} \tag{4}$$

The stochastic differential equations can be related to an Eulerian (advection-diffusion) process by considering the probability density function $p(x,t|x_0,t_0)$, which gives the transition probability $p(x,t|x_0,t_0)dx$ of X_t from the value x_0 at t_0 into the interval $(x, x+dx)$ at t. This probability density function can be obtained by solving the Fokker-Planck equation. The Fokker-Planck equation for the advection diffusion process becomes (Risken,1984):

$$\frac{\partial p}{\partial t} = -\frac{\partial}{\partial x_i}\left(f_i(t, x_i)\, p \right) + \frac{1}{2}\frac{\partial^2}{\partial x_i \partial x_j}\left(g_{ij}^2(t, x_i)\, p \right) \tag{5}$$

The drift function and noise function from the sde (equation 1) can be determined from the Fokker-Planck equation (equation 4) in such a way that it corresponds to the advection-diffusion process (equation 3):

$$f_i(t_i, x_i) = u_i + \frac{\partial D}{\partial x_i} \qquad g_i(t_i, x_i) = \sqrt{2D} \tag{6}$$

The underlying sde that describes the advection-diffusion process is then equal to:

$$dX_{i,t} = \left(u_i + \frac{\partial D}{\partial x_i} \right) dt + \sqrt{2D}\, dW_{i,t} \tag{7}$$

An additional term shows up in the drift term, representing the gradient of the diffusion coefficient. Without this term, particles will accumulate in regions with low diffusion, which is unphysical. Therefore, a transport term equal to the gradient of the diffusion needs to be included in the particle displacement function. For the numerical implementation, we separated the sde equation into an advection part and a diffusion part. For the advection part, the equation for the particle displacement then collapses to a deterministic differential equation. For the diffusion part, we took the sde (equation 7) without the term u_i, which represents a Fickian diffusion process.

2.2 Numerical schemes for particle tracking routine

For the advection induced displacement of a particle, the following equation needs to be solved:

(8) $$\frac{dx_i}{dt} = u_i$$

The most straightforward numerical scheme is the Euler scheme, which uses the velocity at the previous time step to calculate the new position. However, the Euler scheme may lead to inaccurate results (Wols et al., 2010). Therefore, a fourth order Runge-Kutta scheme is used to solve the advection displacement.

Different schemes are available that approximate the stochastic differential equation for the Fickian diffusion process. The schemes were derived from a stochastic Taylor expansion of the underlying sde (Stijnen, 2002; Charles, 2007). Adding up more terms of the Taylor expansion leads to more accurate schemes.

The Euler scheme is relatively straightforward and includes only first-order terms. The new position of the particle due to diffusion is given by:

(9) $$Y_{n+1} = Y_n + f(t_n, Y_n)\Delta t + g(t_n, Y_n)\Delta W_n$$

For the Fickian diffusion process, the Euler scheme becomes:

(10) $$Y_{n+1} = Y_n + \frac{dD}{dx}\Delta t + \sqrt{2D}\Delta W_n$$

A higher order scheme is the Milstein scheme, where the second-order terms of the stochastic Taylor expansion are included (Platen en Kloeden, 1992). The new position of the particle then yields:

(11) $$Y_{n+1} = Y_n + f(t_n, Y_n)\Delta t + g(t_n, Y_n)\Delta W_n + \frac{1}{2} g(t_n, Y_n)\frac{\partial g}{\partial x}\left(\left(\Delta W_n\right)^2 - \Delta t\right)$$

For the Fickian diffusion process, the Milstein scheme becomes:

(12) $$Y_{n+1} = Y_n + \frac{dD}{dx}\Delta t + \sqrt{2D}\Delta W_n + \frac{1}{2}\frac{dD}{dx}\left(\left(\Delta W_n\right)^2 - \Delta t\right)$$

The combined displacement of the particles consists of the advection displacement and diffusion displacement (equation 12).

3. Implementation in COMSOL

The particle tracking routine uses the resolved flow fields from a COMSOL Multiphysics computation. A turbulent flow model (using the *k-ε* turbulence model) is solved in COMSOL v3.5a. A Matlab routine is developed to calculate the particle displacements using the results of the COMSOL calculation. The resolved velocity fields (*u, v* and *w*) are used to determine the advection step, whereas the resolved turbulent kinetic energies (*k*) and dissipation (*ε*) are used to determine the diffusion step. The diffusion coefficient is then equal to:

(13) $$D = C_\mu \frac{k^2}{\varepsilon}$$

where C_μ is a constant in the k-ε model.

The performance of ozone systems is determined by recording the amount of dissolved ozone exposed to each particle, which results in a distribution of ozone exposures (CT-values). The (dissolved) ozone concentration is determined in COMSOL by the advection-diffusion model, where the decay of ozone is modelled as a first-order decay.

4. Results

4.1 Test case: wall treatment

A challenge for diffusion schemes is to prevent particles from unrealistically crossing a closed wall. The two numerical schemes were therefore examined for a simple case with a non-uniform diffusion field. A two-dimensional square domain (40x40 elements) was chosen. In Figure 1 on the left, the noise term (*g*) is displayed. The diffusion was set to zero on the outer ring of the domain, so that $x=\pm L/2$ and $y=\pm L/2$ acted as virtual walls. Particles were not allowed to enter the outer region bounded by these virtual walls. In Figure 1 on the right, the drift term (*f*) is shown, which prevents the particles from accumulating at regions with low diffusion. Two different types of white noise were investigated: Gaussian white noise and uniform white noise, both processes had a random increment with mean zero and variance one. A total number of 1000 particles were released at the centre of the domain. The particles positions after 1000 time steps of $\Delta t=0.1$ s are shown in Figure 2. The particles

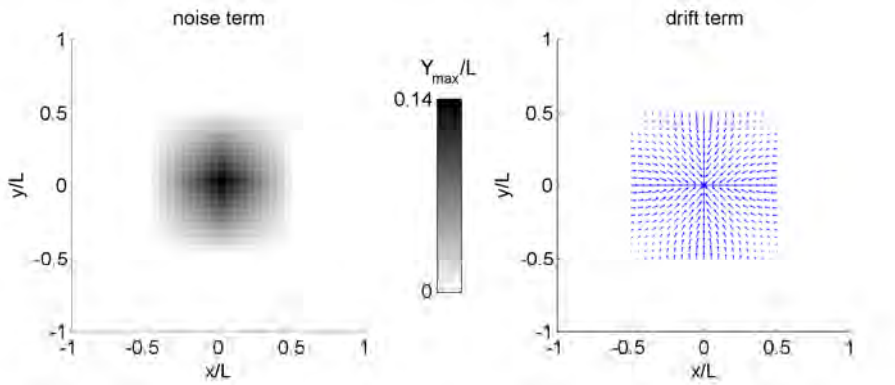

Figure 1 Left panel: Non-uniform diffusion coefficient (maximum displacement of a particle in one step is given by: $Y_{max}=\sqrt{(2D_{max}\Delta t)}$). In the outer region, the diffusion was set to zero to simulate a wall. Right panel: Drift term corresponding to the diffusion field.

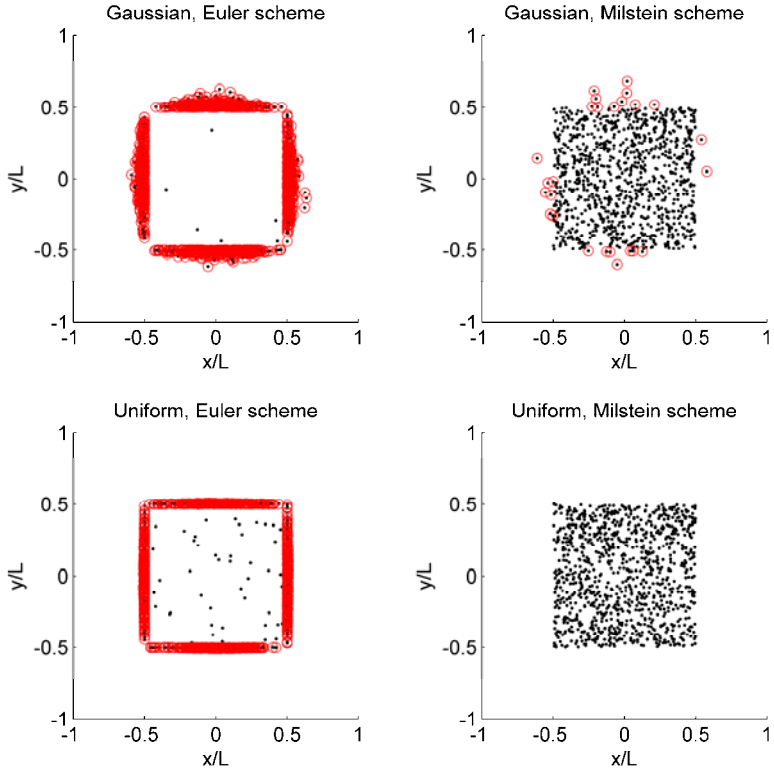

Figure 2 Particle distributions (in 2D) for different numerical schemes. The particles that had moved through the virtual walls are highlighted by a red circle.

that had moved through the virtual walls are highlighted by a red circle. For the Euler scheme, almost all the particles had crossed the walls. The results were much better for the Milstein scheme. Using the Gaussian white noise a few particles had crossed the wall due to large increments in the Gaussian process, whereas using the uniform white noise no particles had crossed the wall. In contrast with the Gaussian white noise, for the uniform noise process the random increments are bounded (between $-\sqrt{3}$ and $\sqrt{3}$), so that particles were less likely to cross the wall. Of course, by further raising the time step or diffusion coefficient, particles cross the wall for all the methods, but it still holds that for the uniform white noise, particles are least likely to cross the wall. Using this method with not too large time steps (Courant-Friedrichs-Lewy number

not larger than 1), no special treatment, such as bouncing, is necessary at the wall. Therefore, the uniform white noise in combination with the Milstein scheme was used.

4.2 Test case: diffusion properties

Two test cases were considered to evaluate the diffusion properties of the above mentioned Milstein scheme. A two-dimensional square domain was chosen (40x40 elements). For the first case, the diffusion coefficient was constant in *x*-direction and varied in *y*-direction (Figure 3). The maximum displacement was of the same order of magnitude as the element size. At the walls, the diffusion coefficients were set to zero, so no particles were allowed to cross the walls. Particles were initially uniformly distributed over the domain. The distribution must remain uniform, because there was no concentration gradient. With an inaccurate particle method the particles will accumulate in the regions with lower diffusion and cross the walls. But in the case of the Milstein scheme as implemented in equation 12, the particle distribution should remain uniform. In Figure 3, the particle density in *x*- and *y*-direction is shown at different time steps. The particle distributions remained uniform, confirming that this method prevents particles from accumulating at regions with low diffusion and prevents particles from crossing the wall.

For the second test case, the same domain was chosen, but the diffusion coefficient was set constant over the domain to evaluate the diffusion properties. After an initial release of particles in the middle of the domain, the distribution of particles must spread out according to a Gaussian distribution, given by (in 2D):

$$p(x, y, t) = \frac{M}{\sqrt{4\pi Dt}} \exp\left(-\frac{x^2 + y^2}{4Dt}\right) \tag{14}$$

where M represents the initial mass. The analytical solution as well as the particle distribution are shown in Figure 4. Both distributions coincide, indicating that the diffusion properties were properly addressed by the numerical scheme.

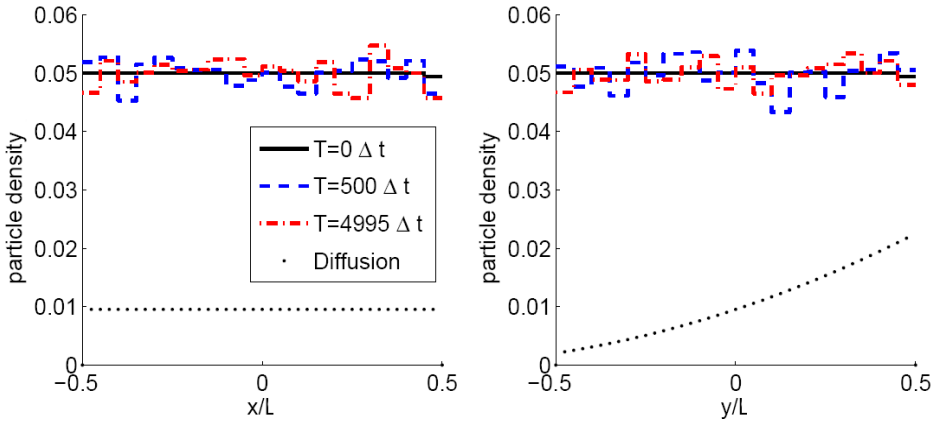

Figure 3 Particle distributions (in 2D) for a non-uniform diffusion coefficient in y-direction (Y_{max}=0.026L, N_p=10 000).

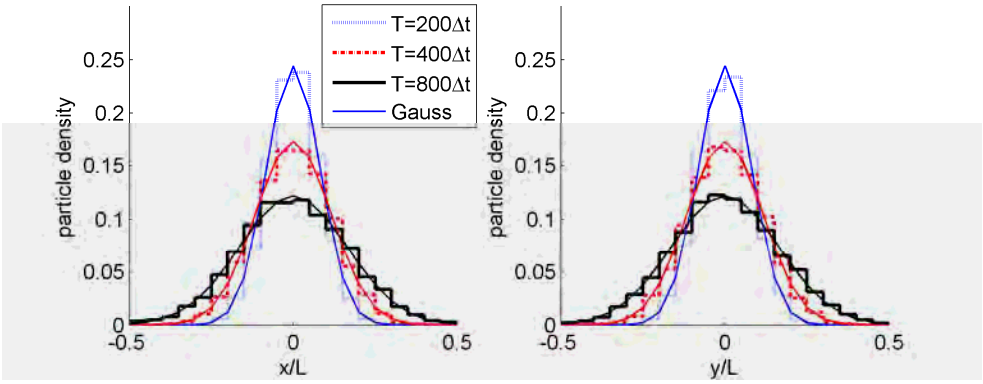

Figure 4 Particle distributions (in 2D) for a uniform diffusion coefficient (Y_{max}=0.01L, N_p=10 000).

4.3 Test case: channel flow

The combination of an advection and diffusion displacement was tested for a simple channel flow, given by Elder (1959). Elder assumed a logarithmic (horizontal) velocity profile over the height ($u(y)$) equal to:

$$u(y) = u_m + \frac{u_*}{\kappa}\left(1 + \ln\left(\frac{y}{h}\right)\right) \quad (15)$$

and a parabolic diffusion profile D(y):

$$D(y) = \kappa u_* y\left(1 - \frac{y}{h}\right) \quad (16)$$

where u_m is the mean velocity (m/s) and u_* is equal to the shear velocity ($u_*=\sqrt{c_f}\,u_m$, [m/s], friction coefficient $c_f=3\cdot10^{-3}$), h represents the water depth and κ represents the Von Karman constant (κ=0.41). Elder used the theory of Taylor (1954) to derive a longitudinal dispersion coefficient (D_L, [m^2/s]):

$$D_L = 5.86 u_* h \quad (17)$$

The spreading in longitudinal direction (averaged over the depth) is reproduced by a Gaussian distribution. The particle distribution over the depth is expected to become uniform after a peak release of particles over the middle of the height.

Particle displacements were simulated for the given velocity and diffusivity profile. A pulse injection of 10 000 particles at x=0 and y=0 (in the middle of the channel) was used. The particle distributions at different time steps are presented in Figure 5. The longitudinal particle positions were corrected with the mean velocity, so that a distribution was formed around the point x-$u_m t$=0. After a while, the particles were uniformly distributed over the depth and approximated to a Gaussian distribution in longitudinal direction. No particles had crossed the wall. The dispersion coefficient converged to the theoretical value of Elder. The test case showed that the particle tracking technique for a combined advection and diffusion problem leads to accurate results.

5. Application

The particle tracking technique was used to calculate the CT-value distribution in ozone contactors. A smaller distribution results in a better disinfection. Various designs of ozone contactors are evaluated. The ozone contactor at the Leiduin WTP of Waternet (Amsterdam Water Supply) was taken as a reference. A flow rate of 2000 m^3/h per contactor was used for the CFD calculations. A configuration without baffles after the bubble column was considered to investigate the effect of the vertical baffles in the reference contactor. Geometries with additional baffles and turning vanes that reduce short-circuiting were also investigated. Besides the contactor systems, a plug flow system was considered, because it

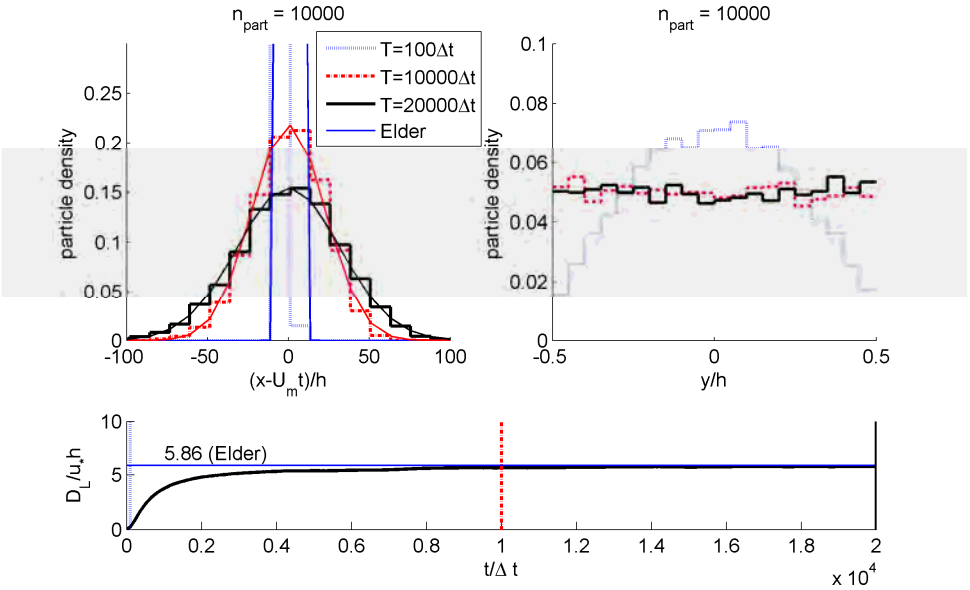

Figure 5 Particle distribution in x-direction and y-direction for a channel flow of Elder (1959), h=0.5 m, Δt=0.2 s.

represents an ideal hydraulic configuration. Comparing the contactors with suboptimal hydraulics to the ideal configuration showed the potential improvement in disinfection capacity. The plug flow was modelled as a flow between two plates (length = 200 m, height = 2 m). The ozone was injected 100 m downstream of the reactor inlet, so the velocity profile between the plates was expected to be fully developed. Mean residence times defined from the injection of ozone to the outlet of the reactor were in the same range as for the baffle contactors. For the reference contactor, the residence times were validated by measurements, reported in Wols et al. (2008).

5.1 Flow fields and ozone concentrations

In Figure 6 on the left, the flow fields are depicted for the contactor variants. For the reference contactor, the velocities increased above and below the baffles. This resulted in regions with high velocities that caused short-circuits. At the fifth baffle, velocities were even higher, because this baffle is higher than the other baffles. Flow separation occurred downstream of the baffles resulting in a large recirculation zone. In the case of no baffles a very large recirculation zone developed that occupied the complete contactor. The high velocities underneath the baffle were reduced by the shear layer that had spread out over the height. Additional baffles reduced the strength of the large recirculation zones as well as the strength of the short-circuit flows. The turning vanes had similar effects.

In Figure 6 on the right, the ozone concentrations for a decay coefficient of $2.5 \cdot 10^{-3}$ s are depicted. By assuming a complete mixing between (dissolved) ozone and water after the bubble column, a uniform (dissolved) ozone distribution underneath the baffle upstream was set as an initial condition. Increasing the number of baffles and therefore reducing the size of the recirculation zones resulted in a more uniform distribution of the dissolved ozone in the contactor.

5.2 CT-value

A number of 5000 particles were released instantaneously at the inlet. While the particles moved towards the outlet of the contactor, the ozone exposure of each particle accumulated until the end of the installation was reached. In Figure 7, the particle trajectories of a particle with the lowest ozone exposure and an average ozone exposure are shown. The combination of diffusion (random displacement) and advection can be clearly seen form the particle trajectories. The accumulated CT-value of the particle is indicated by the colour. The micro-organisms with the lowest ozone exposure are critical for disinfection.

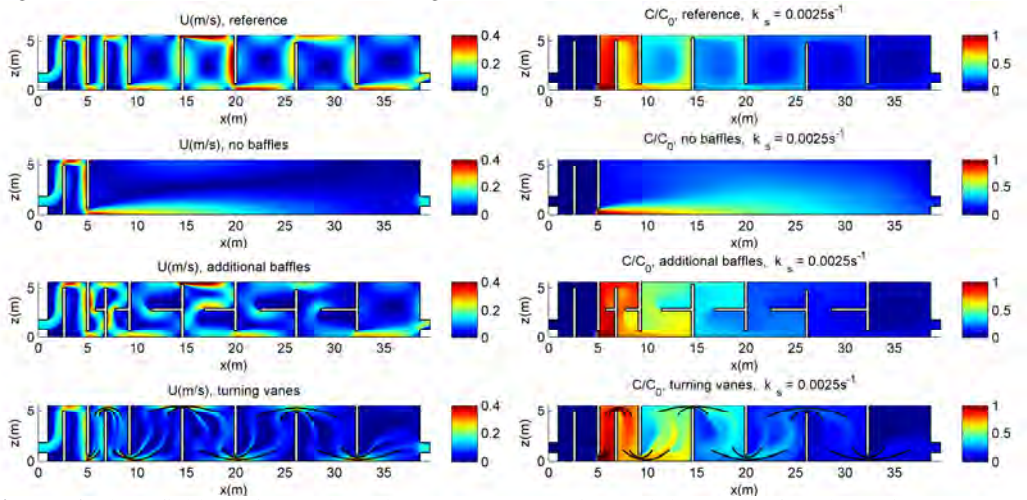

Figure 6 Flow fields (left panel) and ozone concentrations (right panel) for alternative contactor geometries.

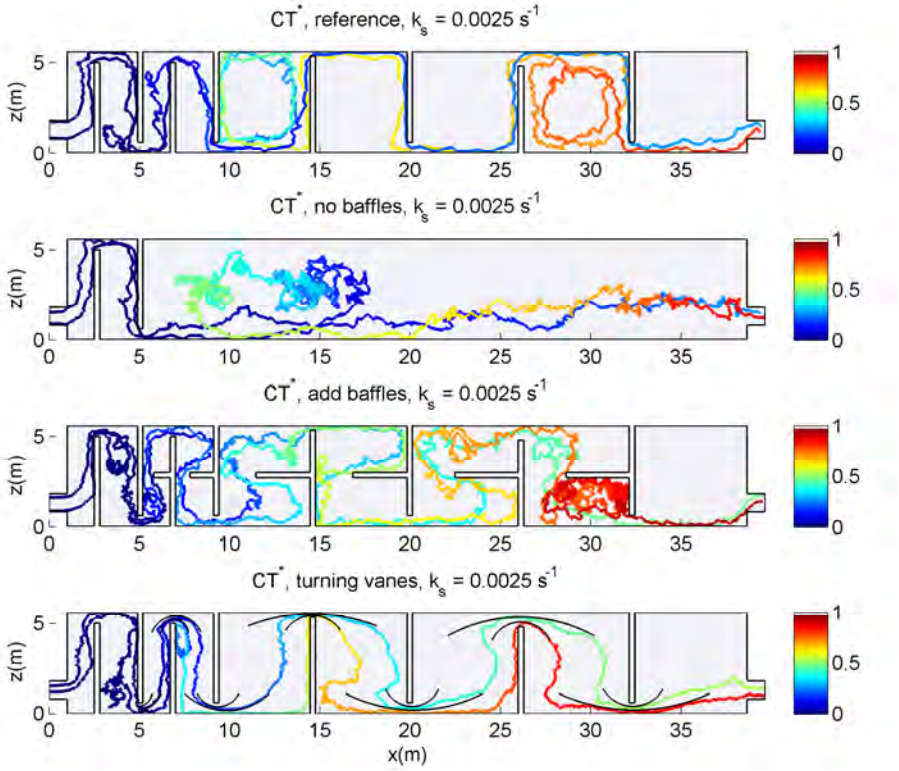

Figure 7 Particle tracks that represent the movements of micro-organisms inside the different contactors. The CT* (dimensionless ozone exposure) is indicated by the colour. For each contactor variant, the two tracks with the lowest and mean CT value are provided.

The CT value was recorded for every particle reaching the outlet, from which a distribution of CT values was constructed (Figure 8). The distribution of CT values provided a complete overview of the performance of these ozone contactors. For the geometry without baffles, a peak occurred at the smallest CT values, caused by the (large number of) particles that left the contactor quickly through short-circuiting. High CT values developed for particles that were trapped inside the large recirculation zone. For the reference configuration a narrower CT value distribution developed: the peak occurred at higher CT values, although the distribution was still asymmetrical and had a large tail at higher CT values. Improving the hydraulics by adding baffles or turning vanes narrowed the CT value distribution and shifted the peak towards a higher CT value. The distribution of CT values was obviously the narrowest for the plug flow configurations.

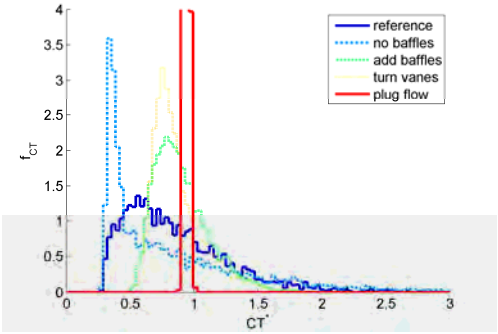

Figure 8 Distribution of normalised CT values obtained from the ozone exposures of the particles at the end of the contactor (k_s=2.5·10^{-3} s^{-1}).

6. Conclusions

A particle tracking technique has been developed to determine the movements of micro-organisms in drinking water treatment installations. The theory of stochastic differential equations is applied to determine the displacement equations of the particles. The particle movements obey the advection-diffusion process, whereby unphysical behaviour – particles crossing solid walls, or accumulating at regions of low diffusion – is prevented. The particle tracking technique is implemented in a Matlab routine, that uses the velocity fields and turbulence properties of the k-ε turbulence model of COMSOL Multiphysics.

The particle tracking technique is useful for modelling disinfection processes in drinking water treatment, since the particles represent individual micro-organisms. Therefore, the design of ozone contactors is optimized using these modelling techniques. It can be concluded that by changing the geometry of the ozone installations – adding horizontal baffles or turning vanes – the lowest ozone exposures (CT-values) are increased, resulting in a more efficient design of these installations.

References

Einstein, A. (1905). Uber die von der molekularkinetischen Theorie der Wärme geforderte Bewegung von in ruhenden Flüssigkeiten suspendierten Teilchen. *Annalen der Physik*, 322 (8):549-560.

Baldyga, J., and Orciuch, W. (2001). Barium sulphate precipitation in a pipe – an experimental study and CFD modelling. *Chemical Engineering Science*, 56:2435-2444.

Brown, R. (1829). Additional remarks of active moleculs. *Philosophical Magazine NS*, 6:161-166.

Charles, W.M. (2007). *Transport modelling in coastal waters using stochastic differential equations.* PhD thesis, Delft University of Technology.

Elder, J.W. (1959). The dispersion of marked fluid in turbulent shear flow. *Journal of Fluid Mechanics*, 5 (4):544-560.

Kloeden, P.E. and Platen, E. (1992). Numerical solution of stochastic differential equations. *Applications of mathematics* vol 23. Springer, Berlin.

Risken, H. (1984). *The Fokker-Planck equation*. Springer series in synergetics 18. Springer, Berlin.

Stijnen, J. (2002). *Numerical methods for stochastic environmental models*. PhD thesis, Delft University of Technology.

Taylor, G. (1954). The dispersion of matter in turbulent flow through a pipe. *Proceedings of the Royal Society of London, Series A, Mathematical and Physical Sciences*, 223 (1155): 446-468.

Wols, B.A. (2010). *CFD in drinking water treatment*, PhD thesis, Delft University.

Wols, B.A., Hofman, J.A.M.H., Uijttewaal, W.S.J., Rietveld, L.C., Stelling, G.S., and van Dijk, J.C. (2008). Residence time distributions in ozone contactors. *Ozone: science & Engineering*, 30(1):49-57.

Zhang J., Huck, P.M., Anderson, W.B. and Stubley, G.D. (2007). A computational fluid dynamics based integrated disinfection design approach for improvement of full-scale ozone contactor performance. *Ozone: science & Engineering*, 29(6):451-460.

Acknowledgements

This work was performed in the TTIW-cooperation framework of Wetsus, centre of excellence for sustainable water technology (www.wetsus.nl) and this work is supported by the joined Dutch Water Supply Companies. Wetsus is funded by the Dutch Ministry of Economic Affairs. The authors would like to thank the participants of the research theme “clean water technology” for the fruitful discussions and their financial support.